Stem Cell Research & Therapy

RESEARCH

Open Access

Human umbilical cord-derived mesenchymal stromal cell exosomes ameliorate aging-associated skeletal muscle atrophy and dysfunction in SAMP10 mice

Zhe Huang[1,2], Limei Piao[1,3*], Xiangkun Meng[1,4*], Aiko Inoue[5,6], Kazuhiro Hitomi[1,7], Hiroyuki Umegaki[6], Masafumi Kuzuya[6,8] and Xian Wu Cheng[1,3,9*]

Abstract

Background Loss of skeletal muscle mass and function in aging individuals is closely linked to physical deterioration and disability. Because exosomes of human umbilical cord-derived mesenchymal stromal cells (hucMSC-Exos) have been widely used to treat various human diseases, we examined their effects on aging-associated muscle atrophy and dysfunction in senescence-accelerated mouse prone 10 (SAMP10) mice, an animal model of human Sarcopenia.

Methods Twenty-four-week-old male SAMP10 mice were randomly assigned to a non-treatment or hucMSC-Exos treatment group.

Results Twelve weeks after intravenous injection of hucMSC-Exos, the treatment group mice showed improvements in skeletal muscle morphology and performance, and elevated levels of the proteins phospho-mammalian target of rapamycin (p-mTOR), myosin heavy chain (MHC), peroxisome proliferator-activated receptor-γ co-activator, and sirtuin1 (Sirt1) in gastrocnemius muscle tissues. HucMSC-Exos also improved muscle mitochondrial biogenesis and lipid drop accumulation in the gastrocnemius muscles. In in vitro experiments, hucMSC-Exos improved cell viability, senescence, apoptosis, and differentiation in association with induction of molecules related to anti-apoptosis (Bcl-2), differentiation (myogenin, MyoD1, myogenic factor-5, and myogenic factor-6), and protein anabolism (p-mTOR, MHC, Sirt1, phospho-AMP-activated protein kinase, phosphor-extracellular signal-regulated kinase1/2, and glycogen synthase kinase3alpha/beta) in C2C12 cells under our experimental conditions.

Conclusions Our findings indicate that hucMSC-Exos treatment ameliorated skeletal muscle atrophy and dysfunction via mitochondrial biogenesis, anti-apoptosis, and protein anabolism mechanisms that might be dependent on an mTOR and Sirt1/PGC1α signaling pathways, indicating that hucMSC-Exos may have promise as a treatment for the management of aging-related frailty and sarcopenia.

Keywords Sarcopenia, Frailty, Mesenchymal stromal cell, Exosomes, Apoptosis, Anabolism

*Correspondence:
Limei Piao
42226925@qq.com
Xiangkun Meng
xkmeng@yeah.net
Xian Wu Cheng
chengxw0908@163.com
Full list of author information is available at the end of the article

Introduction

Sarcopenia and frailty, recognized as chronic muscle disorders by the World Health Organization, are characterized by aging-related skeletal muscle mass loss and dysfunction and result in disability and reduced quality of life [1, 2]. The causes of both muscle diseases are multifactorial and involve both biological and environmental factors, especially sex hormone imbalance, inflammatory actions, oxidative stress, mitochondrial dysfunction, and apoptosis in the skeletal muscle tissues [3–5]. In this context, several therapeutic strategies, including treatments using stem cells, growth factors, hormones, and pharmacological therapeutics, have been adopted in attempts to ameliorate the aging-associated degenerative loss of muscle mass and function.

Although exercise training is known to be the most effective prophylactic against aging-related muscle atrophy in humans and animals [5–7], exercise is impractical or inefficient for elderly individuals with reduced mobility [8–10]. Pharmacological interventions have been used to prevent the development of chronic skeletal muscle diseases such as sarcopenia, generally via supplementation of hormones (including sex and growth hormones) and myoprotein, but these therapies often have adverse side effects [11–13]. There is thus an urgent need for the development of effective alternatives based on the molecular mechanisms of aging-associated sarcopenia.

Mesenchymal stromal cells (MSCs) obtained from various adult tissues—e.g., adipose tissue, umbilical cord tissue, or bone marrow—have been applied for the regeneration of skeletal muscle and other tissues [14–16]. Such MSC treatment is effective for ameliorating age-associated muscle atrophy and dysfunction, possibly by modulating anti-inflammatory, anti-apoptosis, and paracrine growth signaling (for review see Trapana et al. [17]). Although only two decades ago the human umbilical cord was considered medical waste, more recently it has become a promising cell source in regenerative medicine due to the distinct multilineage differentiation capacity of human umbilical cord-derived MSCs (hucMSCs). HucMSCs exhibited faster proliferation and higher migration potency toward activated or non-activated lymphocytes than bone marrow- and adipose tissue-derived MSCs [18]. HucMSCs has also been shown to be useful in patients with steroid-resistant with acute graft-versus-host disease [19].

Exosomes, small extracellular vesicles of 40–160 nm diameter, have been garnering increasing interest in regenerative medicine [20]. In adult mice, exosomes play essential roles in the repair of numerous tissues, including heart, muscle and vascular tissues [21–23]. Bone marrow mesenchymal stem cell-derived exosomes have been shown to promote muscle satellite cell activation and skeletal muscle regeneration via the miR-210-3p/KLF7 mechanism [21]. Limited laboratory studies reported that hucMSC-derived exosome (hucMSC-Exos) can produce an acute beneficial effect on several tissue injuries and regenerations [24–27]. Exosomes are key transmitters of multi-biological signals, which are important for intercellular communication under physiological and pathological conditions. The therapeutic potential of hucMSC-Exos in aging-related chronic muscle disease remains uncertain. In this study we investigated the ability of hucMSC-Exos to reverse the loss of skeletal muscle mass and function in senescence-accelerated mouse prone 10 (SAMP10) mice.

Materials and methods

Antibodies

Antibodies against the following proteins were used in this study: t-Akt (total protein kinase B, #2967); phospho-Akt^{s473} (p-Akt^{s473}, #4060); t-AMPK [total adenosine monophosphate (AMP)-activated protein kinase alpha, #2793]; phospho-AMPKα^{thr172} (p-AMPKα^{thr172}, #2531); t-Erk1/2 (total-extracellular signal-regulated kinase1/2, #9107); t-GSK3α/β (total-glycogen synthase kinase 3alpha/beta, #5676); phospho-GSK3α/β$^{s21/9}$ (p-GSK3α/β$^{s21/9}$, #9331); phospho-Erk1/2$^{thr202/tyr204}$ (p-Erk1/2$^{thr202/tyr204}$, #4377); t-mTOR (total mammalian target of rapamycin, #4517); phospho-mTOR^{s2448} (p-mTOR^{s2448}, #2971); Bax (Bcl-2-associated X protein, #2772); Bcl-2 (B-cell lymphoma 2, #2870); Sirt1 (Sirtuin 1, #D1D7); rabbit mAb (#9475) (all from Cell Signaling Technology); phospho-S6 ribosomal protein (p-S6R, Ser235/236) (D57.2.2E) XP Rabbit mAb (CTS; 4858), Anti-Ki67 antibody [B56] (Abcam; ab279653), PGC1-α (peroxisome proliferator-activated receptor gamma coactivator-1-alpha; Abcam, #ab54481); MHC (myosin heavy chain; R&D, #MAB4470); Myogene (R&D, #MAB6686); MYF-5(R&D, #MAB4027); anti-CD9 (#015-27771); anti-CD63 (#016-27061); anti-CD81(#018-27761); and anti-GAPDH (#015-25473) (the latter 4 antibodies were from Wako). The following secondary antibodies were also used: anti-rabbit IgG HRP conjugate (GE) and anti-mouse IgG HRP conjugate (GE).

Cell culture

The hucMSCs used in all of our experiments were the kind gift of The Cord Blood/Umbilical Cord Bank of the Affiliated Hospital of the Institute of Medical Sciences, University of Tokyo (IMSUT CORD, Tokyo). The hucMSCs were cultured in serum-free CiMS-BM medium (#A2G00P05C; Nipro, Osaka, Japan) [16]. C2C12 cells were from the American Type Culture Collection and were cultured in Dulbecco's Modified Eagle Medium (DMEM) supplemented with 10% fetal bovine serum

(FBS). For C2C12 myoblast differentiation, cells were cultured in 2% horse serum/DMEM at 37 °C in 5% CO2. The C2C12 cells were replenished with fresh differentiation medium every 24 h. After 5–7 days of differentiation, the myoblasts had lengthened, fused, and became multinucleated myotubes [28].

Exosome isolation from hucMSCs

The hucMSCs were cultured in serum-free CiMS-BM medium for 48 h and were subjected to exosome isolation. The cell supernatants were centrifuged for 10 min (2000 g) to exclude the cellular debris, and then centrifuged again for 30 min (10,000 g) and filtered through a 0.22-μm filter. The isolated supernatant was then ultracentrifuged for 70 min (100,000 g) and the sediment was rinsed twice with phosphate-buffered saline solution (PBS), and ultracentrifuged for 70 min at 100,000 g. Following resuspension in 0.5 ml of PBS, the exomes were kept at 4 °C until further use and analysis. The number and size of the exosomes were examined using a NanoSight LM10 system (NanoSight). The protein and particle concentration were quantified by the bovine serum albumin (BSA) method and nanoparticle tracking analysis, respectively. In brief, we resuspend exosome pellet in 200 μl RIPA buffer containing appropriate protease inhibitor cocktail. Following vortex for 15 s and incubation on ice for 5 min to allow complete lysis, the exosome protein concentration was then detected by protein assay kit according to the instruction of manufacturer. The sample was subject to western blot assay.

Exosome protein labeling

C2C12 cells were seeded (1.25×10^4 cells/well) on a 4-well chamber slide and cultured at 37 °C overnight. The exosomes (10 μg of protein or 1×10^8 particle count) from hucMSCc were labeled using an ExoSparkler Exosome Membrane Labeling Kit (DOJINDO, #344-09691), and were applied to each well. The C2C12 cells were cultured for 4 h and the cells were observed using a fluorescence microscope.

Cell imaging

C2C12-EGFP cells were treated with exosomes for 24 h. The cells were then plated in new differentiation medium, and visualized and captured under the LSM5 880 (Zeiss) confocal microscope at the indicated times. Quantification of the mean myotube diameter was performed by IMARIS software.

Cell proliferation assay

C2C12 cells were seeded onto 96-well plates, and 24 h later the cells were treated with exosomes for 24 h. Twenty microliters/well of CellTiter 96 Aqueous One-Solution Reagent (Promega) was added to each well of the 96-well plates, and the plates were cultured for 3 h at 37 °C. The absorbance was determined at 492 nm using a Cytation5 microplate reader (BioTek). Viability was evaluated as the ratio of absorbance of treated cells to untreated cells [29, 30].

TUNEL staining assay

For apoptosis assay, C2C12 cells were seeded onto 4-well chamber slides and left for overnight, and then the cells were treated with 400 μM of H2O2 in presence and absence of hucMSC-Exos for 24 h. The cells were fixed and detected by using a terminal deoxynucleotidyl transferase-mediated dUTP nick end labeling (TUNEL) In-situ Apoptosis Detection Kit (TAKARA, #MK500) for the evaluations of apoptotic cells as described [31].

Senescence induction

To induce senescence by doxorubicin hydrochloride (DXR) (Wako, #040-21521), C2C12 cells were plated on 4-well chamber slides at a density of 1.4×10^4 cells/well, medium containing DXR at 150 ng/ml was added to the chambers, and the C2C12 cells were incubated for 4 days.

SA-β-gal staining and immunocytochemistry

SA-β-gal assay was performed with Fluorometric Cellular Senescence Detection Kit-SPiDER-βGal (Dojindo, SG03, Japan) [32]. The cell senescence was also performed by immunocytochemistry as described [33]. In brief, C2C12 cells were seed in 4-well chamber slides for overnight and were treated with 20 μM of DXR alone or 20 μM of DXR + 20 ng/mL of hucMSC-Exos for 96 h, respectively. And cells were fixed with 4% paraformaldehyde for 5 min and incubated with staining solution mix for 30 min at 37 °C. The cells were then permeabilized with 0.2% Triton-X100 for 10 min and blocked in 5% bovine serum albumin for 30 min at room temperature followed by incubated with the antibodies against p-S6R (1:1000) and Ki67 (1:500) at 4 °C for overnight. Following washing with phosphate buffered saline (PBS) for five times, the cells were then treated with Goat anti-Mouse IgG (H + L) Highly Cross-Adsorbed Secondary Antibody, Alexa Fluor 647 (1:1000, A-21236), or Goat anti-Rabbit IgG (H + L) Cross-Adsorbed Secondary Antibody, Alexa Fluor 405 (1:1000, A-31556), respectively, for 1 h at room temperature. The cells were observed under the LSM5 880 (Zeiss) confocal microscope to determine whether any had turned blue, and the numbers of $Ki67^-p\text{-}S6R^+SA\text{-}\beta\text{-}gal^+$ cells were calculated in four random microscopic sections from three independent fields of each slide, and the percentage of $SA\text{-}\beta\text{-}gal^+$ (blue-stained) cells was presented as the number of these cells per total cells at high-power field (×400).

Animals

Eight-week-old male mice (SAMP10/TaSlc) were provided by Japan SLC (Hamamatsu, Japan). All mice were housed one per cage under standard conditions (23 ± 1 °C, 50 ± 5% humidity) and fed a standard diet for 16 weeks, with a 12-h light/dark cycle in a viral pathogen-free facility. Sixteen-week-old mice with body weights of 25–28 g were subjected to in vivo animal experiments. The animal study protocol (entitled hucMSCs therapy on sarcopenia; No. 2019-31442 approved on March 24, 2019) was approved by the Institutional Animal Care and Use Committees of by the Ethics Committee of Nagoya University and performed in accordance with the Guide for the Care and Use of Laboratory Animals published by the U.S. National Institutes of Health [26, 34]. The mice were monitored throughout the experiment period, and all experimental protocols involving the mice were performed by trained research staff.

HucMSC-exos treatments and tissue collections

Sixteen-week-old male SAMP10 mice were randomly divided into two groups: an exosome treatment group (n = 10) and a control group (n = 10). 20 μg of hucMSC-Exos diluted in 150 μl of PBS or an equal volume of PBS was injected into the tail vein of mice over a short duration. The mice then underwent weekly endurance capacity and grip strength measurements. At 36 weeks of age, the mice were euthanized by given an intraperitoneal injection with an overdose of sodium pentobarbital (50 mg/kg; Dainippon Pharmaceutical, Osaka, Japan) for tissue sampling. And the mice were then perfused with PBS under physiological pressure, and both gastrocnemius and soleus muscles were isolated and stored at −80 °C for biological or histological analysis. In case animal anaesthesia was not used in this study.

Evaluation of grip strength

A animal digital grip strength meter (Columbus, Largo, FL) was used to evaluate the grip strength test once a week after exosome injection [35]. Mice were held by the tail and allowed to grasp a wire grid with the forepaws, and then gently pulled in the opposite direction until they released their grip. The grip strength was measured three times and averaged [35].

Endurance measurement

A motorized rodent treadmill (TMS-M4, MELQUEST: Tokyo Engineering) was used to evaluate running endurance capacity [36]. A mouse was considered fatigued when it was no longer able to continue running on the treadmill [36].

Western blot analysis

C2C12 cells were treated with the exosomes at the indicated times. Protein extracts were prepared using CelLytic-M mammalian cell lysis reagent (Sigma), a protease inhibitor and multiple phosphatase inhibitors (Wako). The lysates were sonicated 3 times for 10 s each time, and then centrifuged and subjected to protein concentration measurement. The extracts were separated by SDS-PAGE and transferred to Immobilon-P transfer membranes (Millipore). The primary antibodies were diluted in 5% skim milk (or 3% BSA for phosphor antibodies) and incubated overnight at 4 °C. Mouse monoclonal anti-GAPDH (Wako; 1:5000) was used as a loading control. After reaction with the primary antibodies, HRP labeled goat anti-mouse or goat anti-rabbit secondary antibodies (1:5000) were applied to the membranes for 1 h at room temperature. Bound-antibody detection was performed with ECL prime (GE) and the membranes were imaged using ChemiDoc (BioRad) [37]. The band intensity was quantified with ImageJ software and normalized to GAPDH.

Electron microscopy

Skeletal muscle tissues were fixed in 2% glutaraldehyde buffer for 24 h, and then fixed with 2% osmium tetroxide. After dehydration and exposure to propylene oxide, the samples were embedded in Epon resin and ultrathin-sectioned at 80 nm using an ultramicrotome. They were stained with 2% uranyl acetate for 15 min. HucMSC-Exos were absorbed onto formvar carbon-coated nickel grids and fixed in 2% glutaraldehyde buffer, and 2% uranyl acetate was used for negative staining. The sections were examined with an electron microscope (JEM-1400Plus; JEOL) at 80 kV and digital images were obtained with a CCD camera. The mitochondrial number and damage were evaluated by the corresponding number of pixels (magnification: 6000×) using Adobe Photoshop CS5 software. A total of 60–80 mitochondrial cross-sections from 4 to 6 sections were examined and averaged for each animal, and distribution diagrams were calculated separately for each group of mice.

Statistical analyses

The values are expressed as means ± standard deviation (SD). Unpaired Student's *t*-tests were used for comparisons of two groups and a one-way analysis of variance (ANOVA) followed by Tukey post hoc tests was used for multiple comparisons of parametric data (three or more groups). The grip strength and endurance were subjected to a two-way repeated-measures ANOVA and Bonferroni post hoc tests. The determination of

muscle functions (grip strength and endurance) and muscle fiber size (H&E staining), and the electron microscopy were performed by two observers in a blind manner, and the values they obtained were averaged. Statistical analysis was performed using GraphPad Prism 6 software. A p value ≤ 0.05 was considered statistically significant.

Results

HucMSC-Exos identification using electron microscopy and fluorescence

Nanoparticle tracking analysis (NTA) is often applied to check the quality of exosomes. As seen in Fig. 1a, the NTA graph presents the relative amounts of exosomes isolated from s cells. HucMSC-Exos was identified by western blotting assay using both antibodies (24 kda and 64 kDa) against exosome marker proteins and transmission electron microscopy was used to identify negative

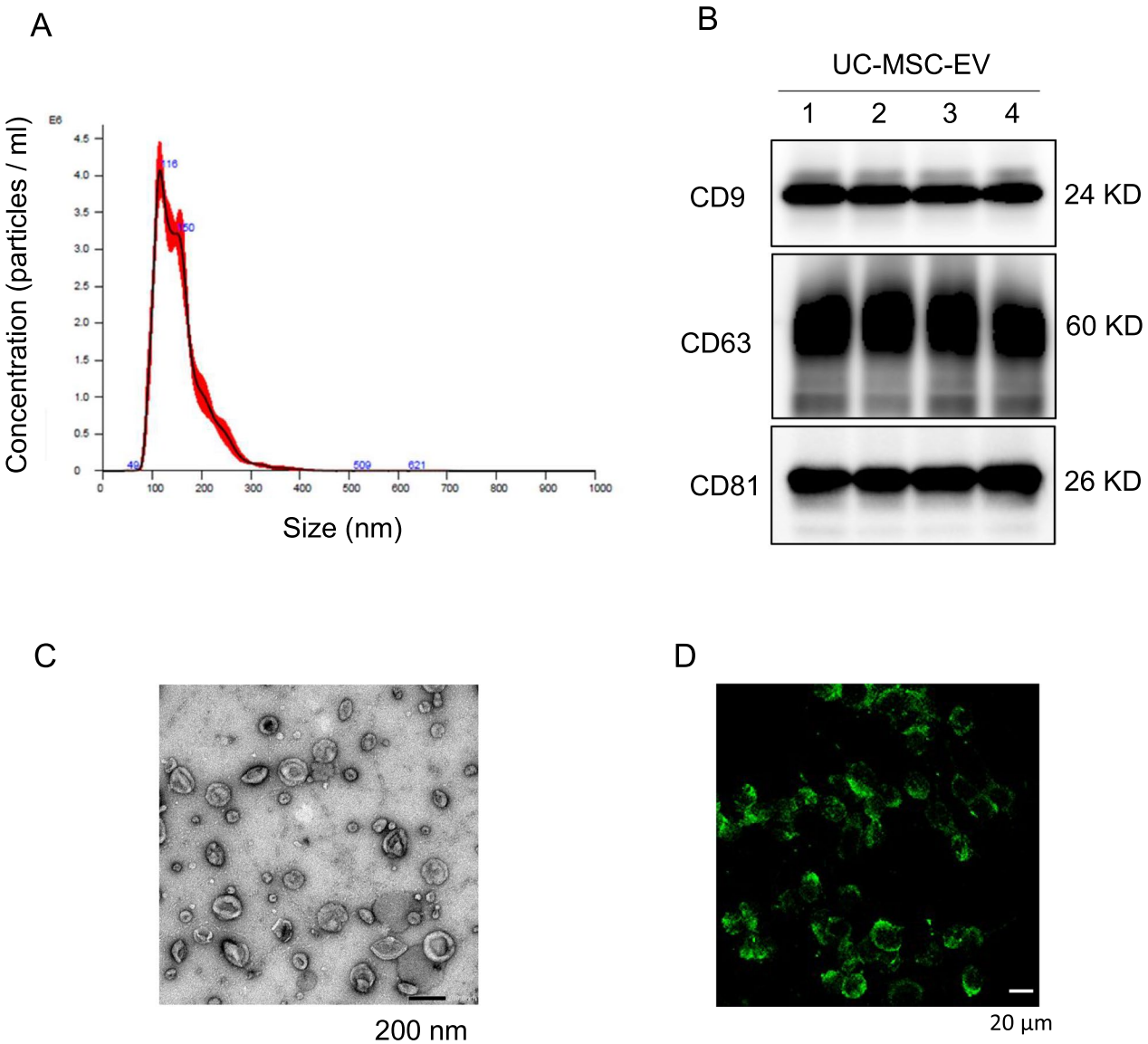

Fig. 1 Isolation of exosomes from hucMSCs. **a** The amounts of exosomes isolated from hucMSCs were examined by nanoparticle tracking analysis. **b, c**. Western blotting using antibodies against exosome marker proteins (**b**) and negative staining under transmission electron microscopy (**c**). **d** Following exosome staining using an ExoSparkler Exosome Membrane Labeling Kit, C2C12 cells were seeded onto a 4-well chamber slides and incubated for 4 h. The cells were observed using a fluorescence microscope

staining (Fig. 1b and c). A fluorescence microscope was used to visualize the exosomes of C2C12 cells (Fig. 1d).

HucMSC-Exos mitigated apoptosis, senescence, and differentiation in C2C12 cells

Several studies have reported that intravenous administration of hucMSC-Exos can lower inflammation, apoptosis, and toxicity in vivo and in vitro [38–40]. Therefore, we treated C2C12 cells with 400 μM of H_2O_2 in the presence and absence of hucMSC-Exos at 20 ng/mL for the indicated durations, and then we examined them by cell viability assay and TUNEL staining. As seen in Fig. 2a–c, hucMSC-Exos administration significantly improved C2C12 cell viability and decreased apoptosis (−38.8%, $p=0.0013$). Quantitative data of SA-β-gal$^+$ staining with Ki67 and pRPS6 antibodies revealed that hucMSC-Exos yielded the same result on C2C12 senescence (decreased β-gal$^+$Ki67$^-$pRPS6$^+$ cells by−38.5%, $p=0.0017$) in response to 150 ng/mL DXR (Fig. 2d, e). As anticipated, it also facilitated C2C12 differentiation (Fig. 3).

HucMSC-Exos positively regulated targeted intracellular signaling pathways in C2C12 cells

In agreement with the phenotype findings, hucMSC-Exos improved harmful changes in the levels of Bcl-2 and Bax in C2C12 cells induced by H2O2 (Fig. 4a, b). HucMSC-Exos upregulated differentiation-related molecules (i.e., myogenin, MyoD1, MYF5, and MYF6) (Fig. 4c, d). In parallel with these effects, hucMSC-Exos enhanced the levels of p-Akt, p-mTOR, p-Erk1/2, p- AMPK, Sirt1 and reduced p-GSK3a/b in C2C12 cells (Fig. 5a, b) and as anticipated, mTOR inhibitor Rapamycin suppressed the levels of p-mTOR, Sirt1, and PGC-1α (Fig. 5c, d).

HucMSC-Exos restored he loss of skeletal muscle mass and function in SAMP10 mice

To explore whether hucMSC-Exos ameliorates muscle atrophy and dysfunction, the tail veins of SAMP10 mice were injected with 20 ug of hucMSC-Exos diluted in 150 μl of PBS, or injected with an equal volume of PBS alone, and then the endurance and grip strength were evaluated at the indicated time points. We observed that hucMSC-Exos treatment significantly improved grip strength (+21.3%, $p=0.013$) and endurance (+17.3%, $p=0.02$) at 36-weeks post-treatment, whereas it had no effect on either parameter at the early time points (28 and 32 weeks) or on body weight throughout the follow-up period (Fig. 6a–c). In agreement with these phenotype findings, hucMSC-Exos increased the weights of the gastrocnemius (+37.6%, $p=0.0014$) and soleus muscles (+30.2%, $p=0.04$) (Fig. 6d, e). The hucMSC-Exos intervention yielded the same results on muscle fiber size (+18.8%, $p=0.014$) (Fig. 6f, g).

The mTOR-signaling pathway participates in hucMSC-Exos-mediated muscle benefits

The mTOR/Akt pathway is a critical intracellular signaling pathway that modulates protein anabolism and growth of the skeletal muscle [28]. To further evaluate the results of hucMSC-Exos-mediated molecular alterations in SAMP10 mice, we performed an immunoblotting assay to evaluate changes in the mTOR signaling pathway. The data of Western blotting showed that the hucMSC-Exos intervention not only elevated the levels of p-mTOR protein, but also stimulated higher-level MHC protein expression in the gastrocnemius muscles of SAMP10 mice compared with that in the non-treated control mice (Fig. 7a, b).

UC-MSCs improved muscle mitochondrial biogenesis and dysfunction

The Sirt1/PGC1α pathway has been shown to participate in mitochondrial biogenesis in vivo and in vitro under various pathological conditions [5, 41]. In our present experiments, the application of hucMSC-Exos enhanced Sirt1 and PGC1α protein expressions in the gastrocnemius muscles of SAMP10 mice (Fig. 7a, b). The electron microscopy demonstrated severe damage in the cristae of mitochondria of the gastrocnemius muscles of the non-treated SAMP10 mice (Fig. 8a). As seen in Fig. 8b, the hucMSC-Exos intervention achieved dramatic reductions in mitochondrial injury (−26.6%, $p=0.026$) and

(See figure on next page.)

Fig. 2 The hucMSC-Exos improved cell viability, senescence, and apoptosis in C2C12 cells in response to H_2O_2 induction. **a**–**c** C2C12 cells were seeded on a 4-well chamber slide and were cultured in 10% fetal bovine serum (FBS)/Dulbecco's modified Eagle's medium (DMEM) overnight. After washing in PBS two times, the cells were cultured for 24 h in serum-free DMEM supplemented with 400 μM of H_2O_2 or with 400 μM of H_2O_2 plus 20 ng/mL of exosomes, and then were subjected to MTT assay to measure cell viability (**a**) and terminal deoxynucleotidyl transferase-mediated dUTP nick end labeling (TUNEL) staining to detect apoptosis (**b**, **c**). Representative images and quantitative data show the viability and apoptosis in the experimental groups. **d, e** C2C12 cells were also cultured for 24 h in serum-free DMEM supplemented with 200 ng/ml of doxorubicin (DXR) or with 20 μM of DXR plus 20 ng/mL of exosomes, respectively, and then were subjected to SA-β-gal, pRPS6, and Ki67 staining to assess senescence. Representative images of the Ki67$^-$pRPS6$^+$SA-β-gal$^+$ cells and quantitative data show the senescence. 100 cells were counted in each group. Data are means ± SD (n = 6–7 for each group), and *P* values were determined by one way ANOVA and Tukey's post hoc tests (A) or Student's *t*-test (**c**, **e**). Scale bars, 10 μm

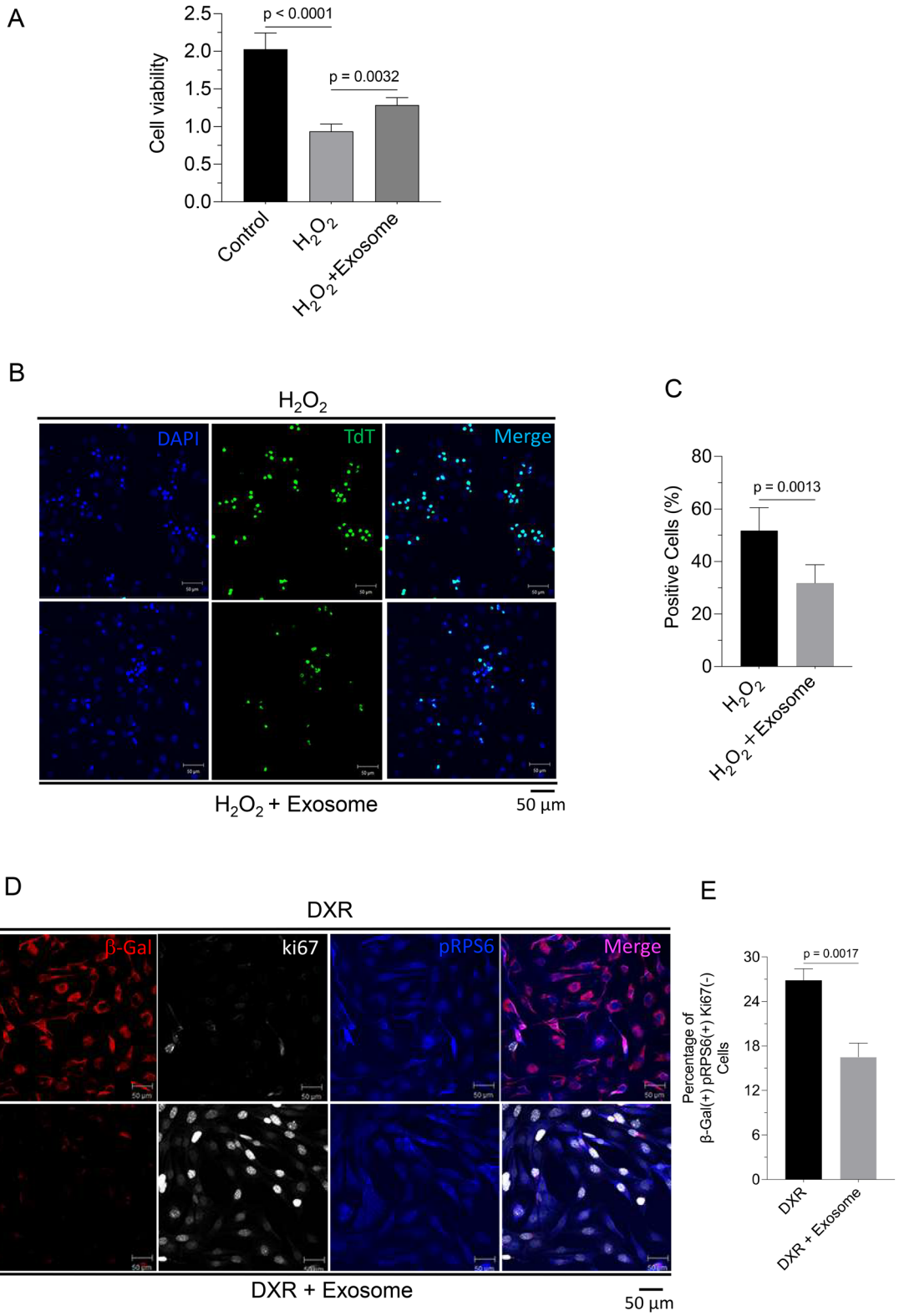

Fig. 2 (See legend on previous page.)

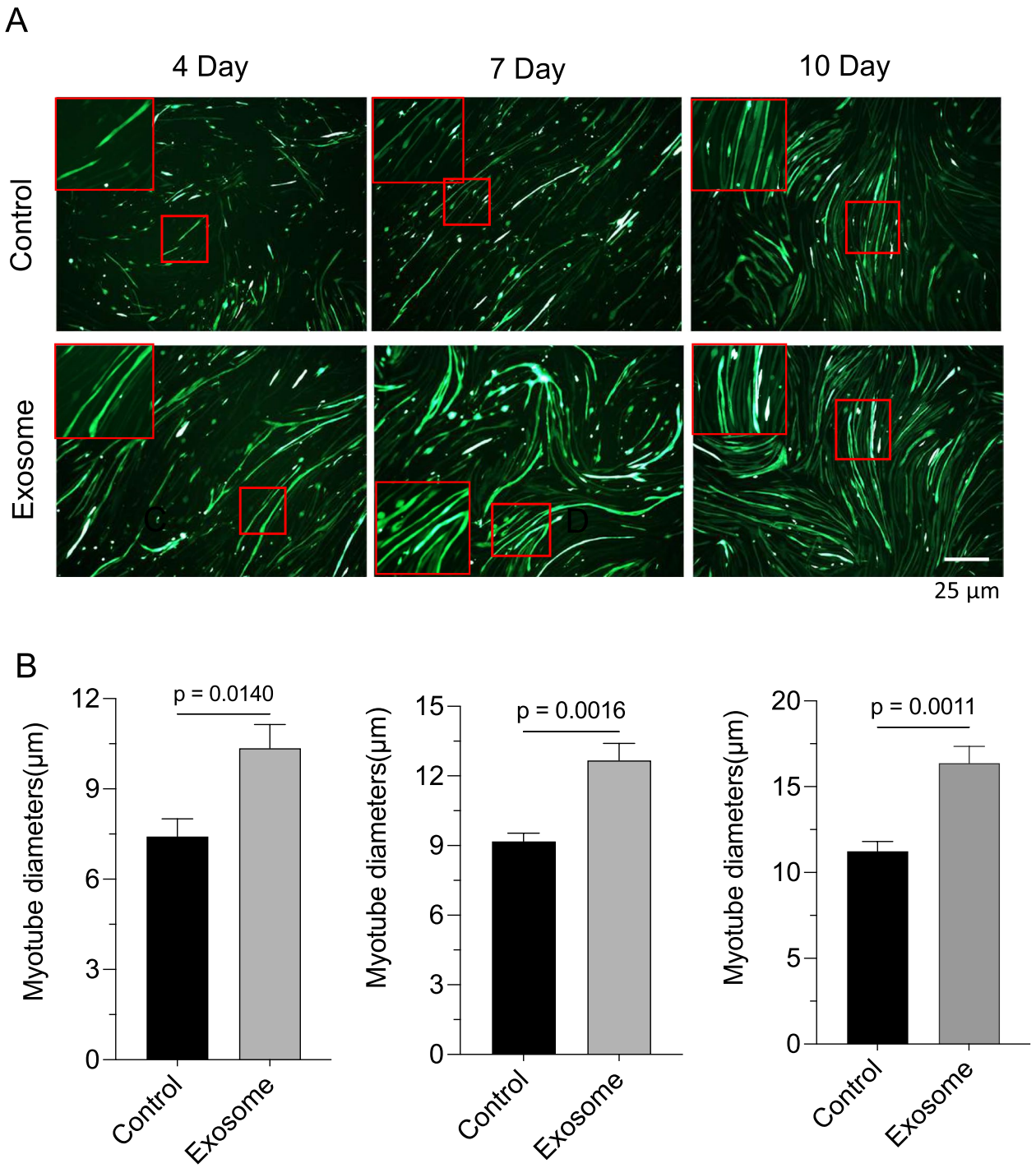

Fig. 3 hucMSC-Exos promote C2C12 cell differentiation. **a, b** C2C12-EGFP cells were seeded on a 4-well chamber slide and were cultured in 10% FBS/DMEM overnight. The cells were cultured in differentiation medium in the presence or absence of exosome solution (20 ng/mL of hucMSC-Exos) for the indicated durations. Representative confocal microscope images (**a**) and quantitative data (**b**) show the myotube diameter at days 4, 7, and 10. Data are means ± SD (n = 6–7 for each group), and *P* values were determined by Student's *t*-test (**b**)

lipid droplet accumulation (−25.3%, $p = 0.011$) compared

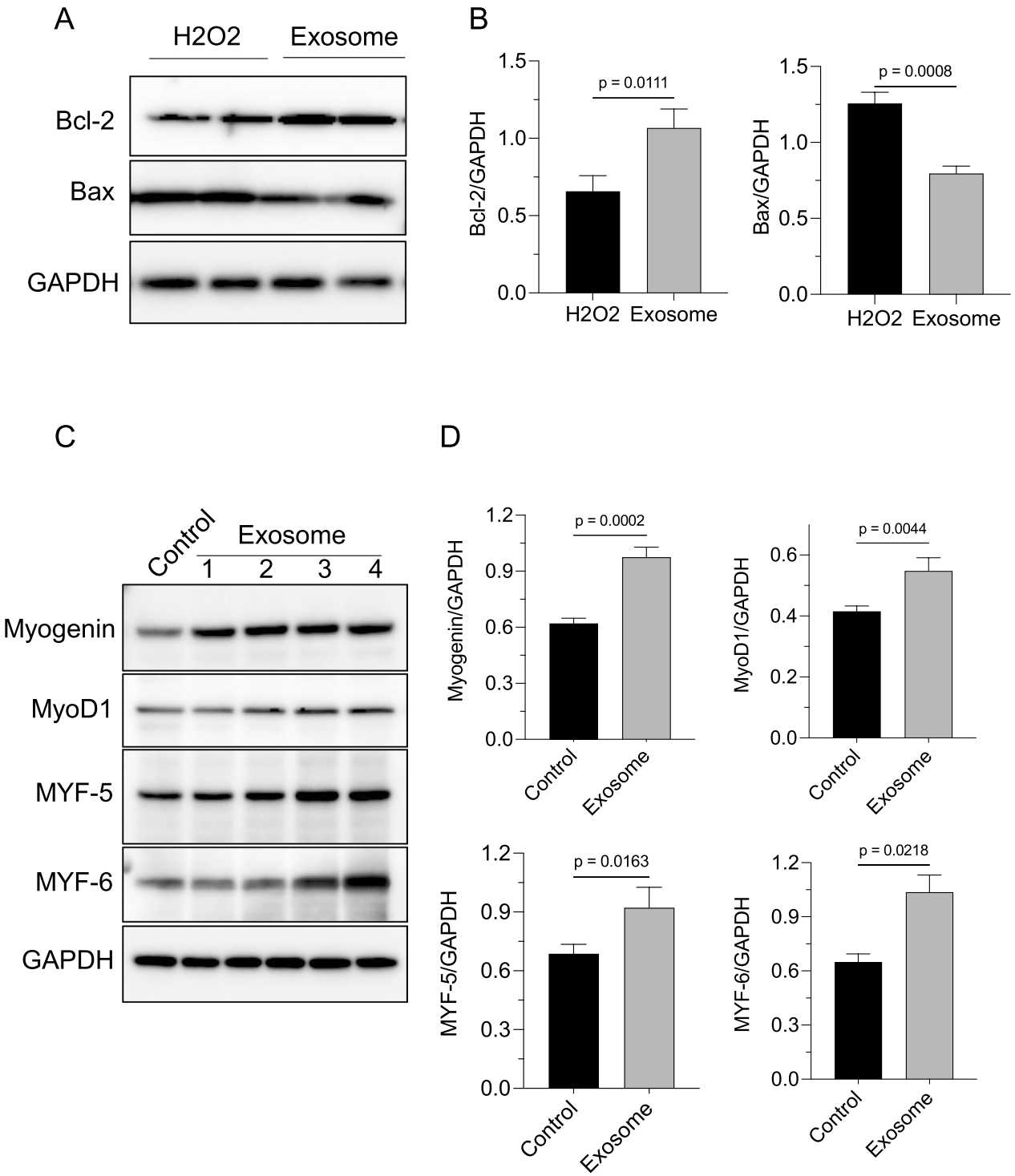

Fig. 4 HucMSC-Exos reduced apoptosis-related protein expressions in C2C12 cells in response to oxidative stress. **a**, **b** C2C12 cells were treated for 24 h with 400 H_2O_2 alone or with 400 μM of H_2O_2 plus 20 ng/mL of exosomes, and then were subjected to western blotting analysis. The band intensities of proteins were quantified and normalized by GAPDH using ImageJ software. **c**, **d** C2C12 cells were cultured in differentiation medium in the presence or absence of exosomes for the indicated amounts of time, and the lysates were analyzed by western blot using the indicated antibodies. Representative western blotting images and quantitative data show the levels of the investigated molecules. Data are means ± SD (n = 3–4 for each group), and P values were determined by Student's *t*-test (**b** and **d**)

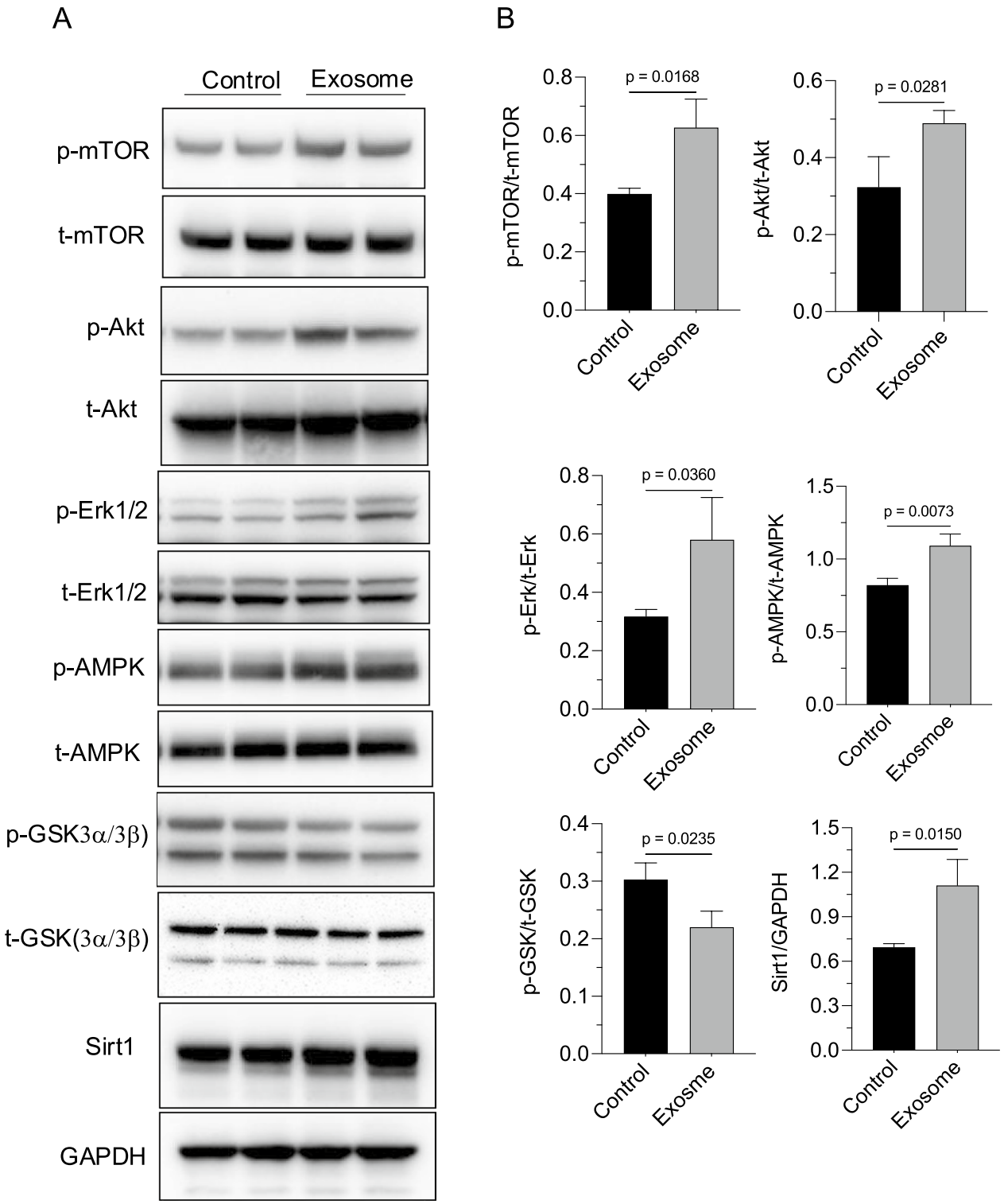

Fig. 5 The effects of hucMSC-Exos on the investigated molecular levels in C2C12 cells. **a, b**: C2C12 cells were treated with or without exosomes for 24 h, and then the lysates were analyzed by western blot. Representative western blotting images and quantitative data show the levels of the investigated molecules (p-mROR, p-Akt, p-Erk, p-AMPKα, p-GSK3α/β, Sirt1). **c**, **d** C2C12 cells were treated with or without rapamycin (100 nM) and/or exosomes for 24 h, and then the lysates were analyzed by western blot using p-mTOR, t-mTOR, PGC-1α, and Sirt1 antibody. Data are means ± SD (n = 4), and P values were determined by Student's *t*-test (**b** and **d**)

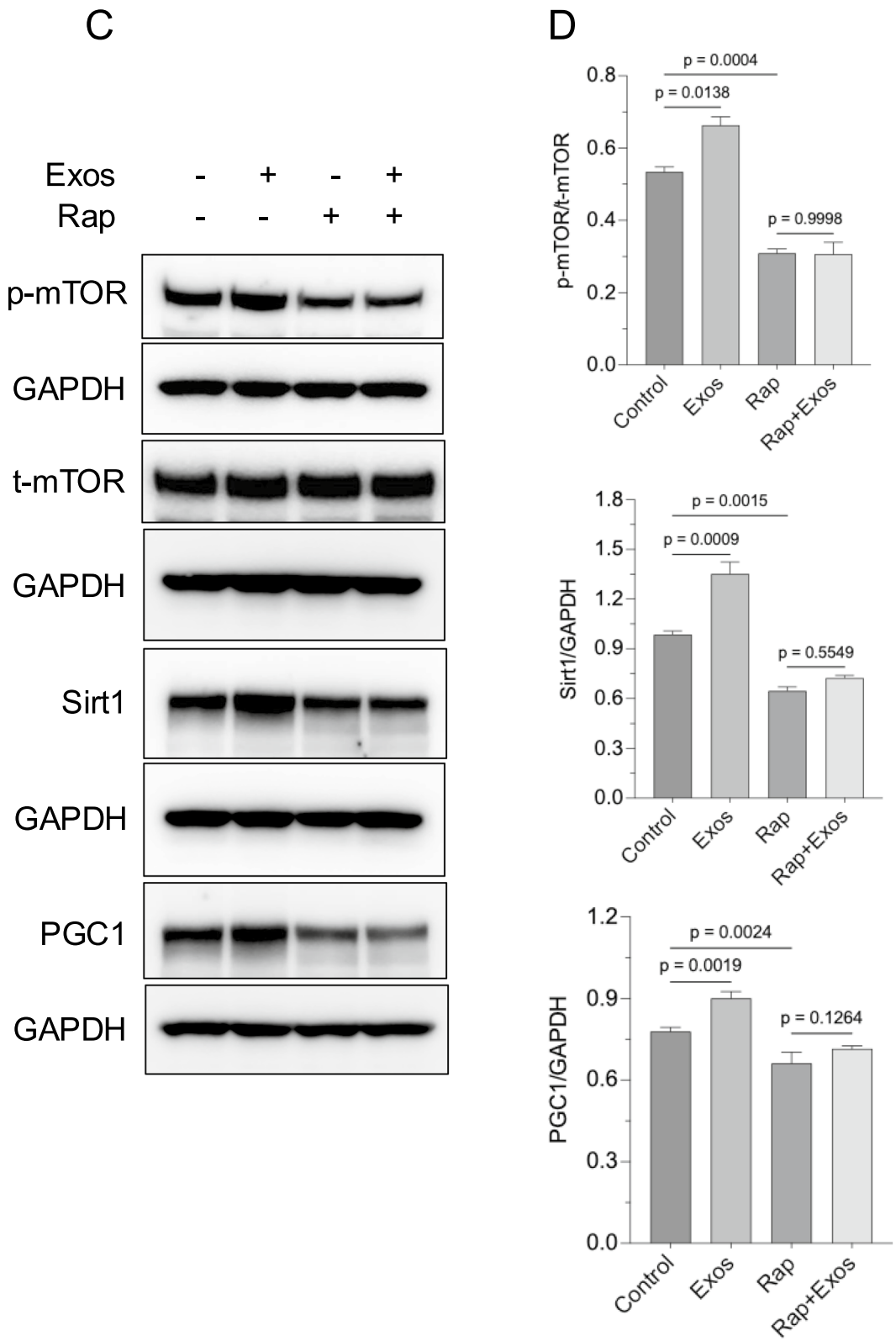

Fig. 5 continued

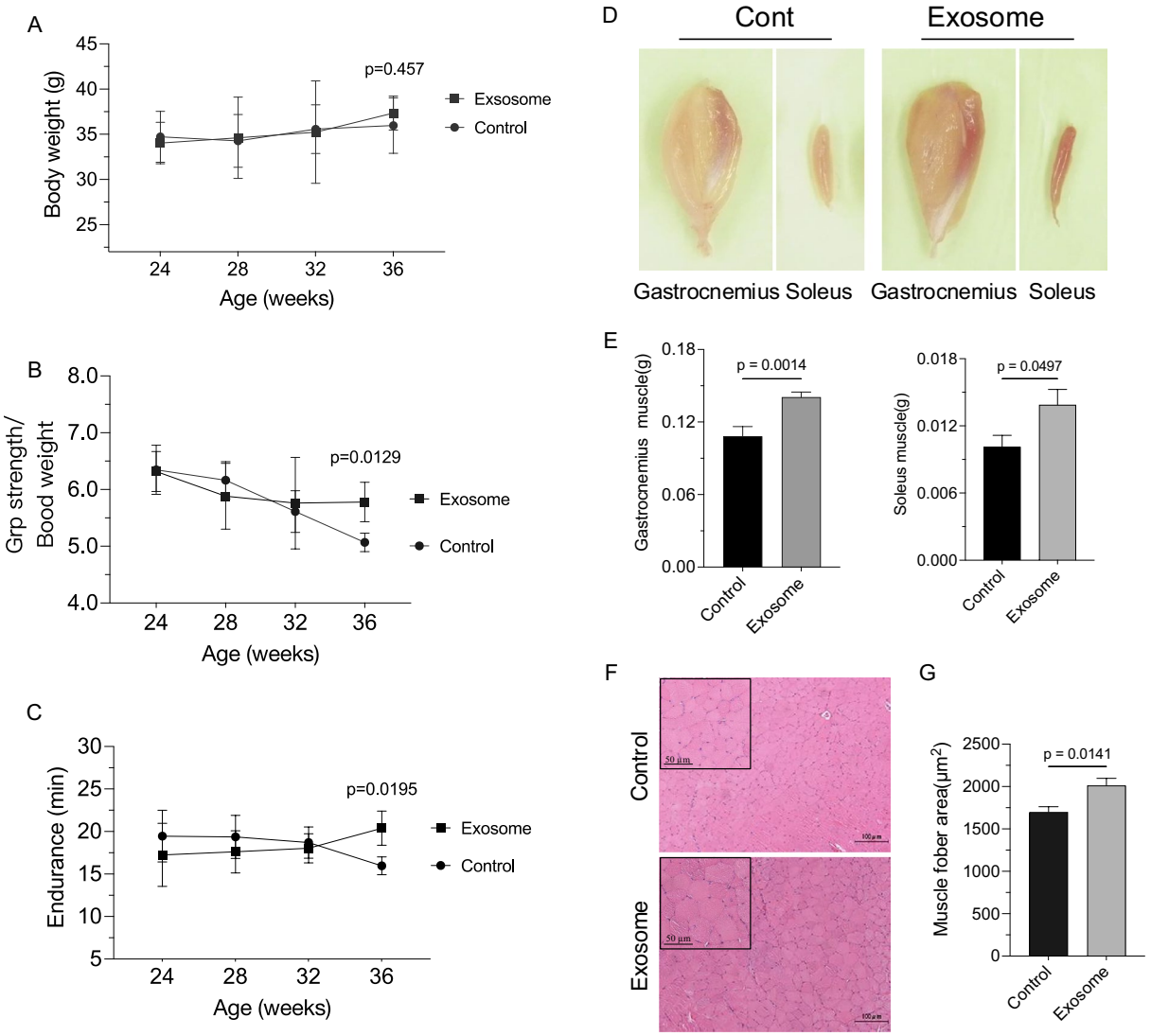

Fig. 6 HucMSC-Exos treatment prevented muscle dysfunction in SAMP10 mice. **a–c** The quantitative data show the body weights (**a**), grip strength/body weight ratios (**b**), and endurance levels (**c**) in both groups at the indicated time points (n = 10 for each group). **d**, **e**: The ratios of gastrocnemius and soleus muscle weights/body weights of the control and exosome-treated mice (n = 10) at 36 weeks after exosome injection. **f, g** Representative HE images and quantitative data for the cross-sections of gastrocnemius muscles from the control and exosome-treated mice at 36 weeks after exosome injection. Data are means ± SD (n = 6–10), and P values were determined by a two-way repeated-measures ANOVA and Bonferroni post hoc tests (**a**–**c**) or Student's *t*-test (**e**, **g**)

to the levels in control mice.

Discussion

Over the past decade, experimental and clinical evidence has indicated the therapeutic potential of hucMSCs for skeletal muscle diseases [42–45]. In this study, we first explored hucMSC-Exos-mediated musculoprotective effects and their potential molecular mechanisms in SAMP10 mice. The most significant finding of our study was that SAMP10 mice administered intravenous hucMSC-Exos were resistant to aging-associated skeletal muscle loss and dysfunction. In vivo, at the molecular and microchange levels, hucMSC-Exos treatment resulted in an increase in the muscle fiber size and the mitochondrial biogenesis associated with the induction of MHC, Sirt1, PGC1α, and p-mTOR proteins in the skeletal muscle tissues in SAMP10 mice. In vitro, hucMSC-Exos treatment improved the cell viability, apoptosis, senescence, and differentiation in association with beneficial changes in the apoptosis (Bax and Bcl-2), differentiation (myogenin, MyoD1, MYF5, and MYF6), and protein anabolism (p-mTOR,

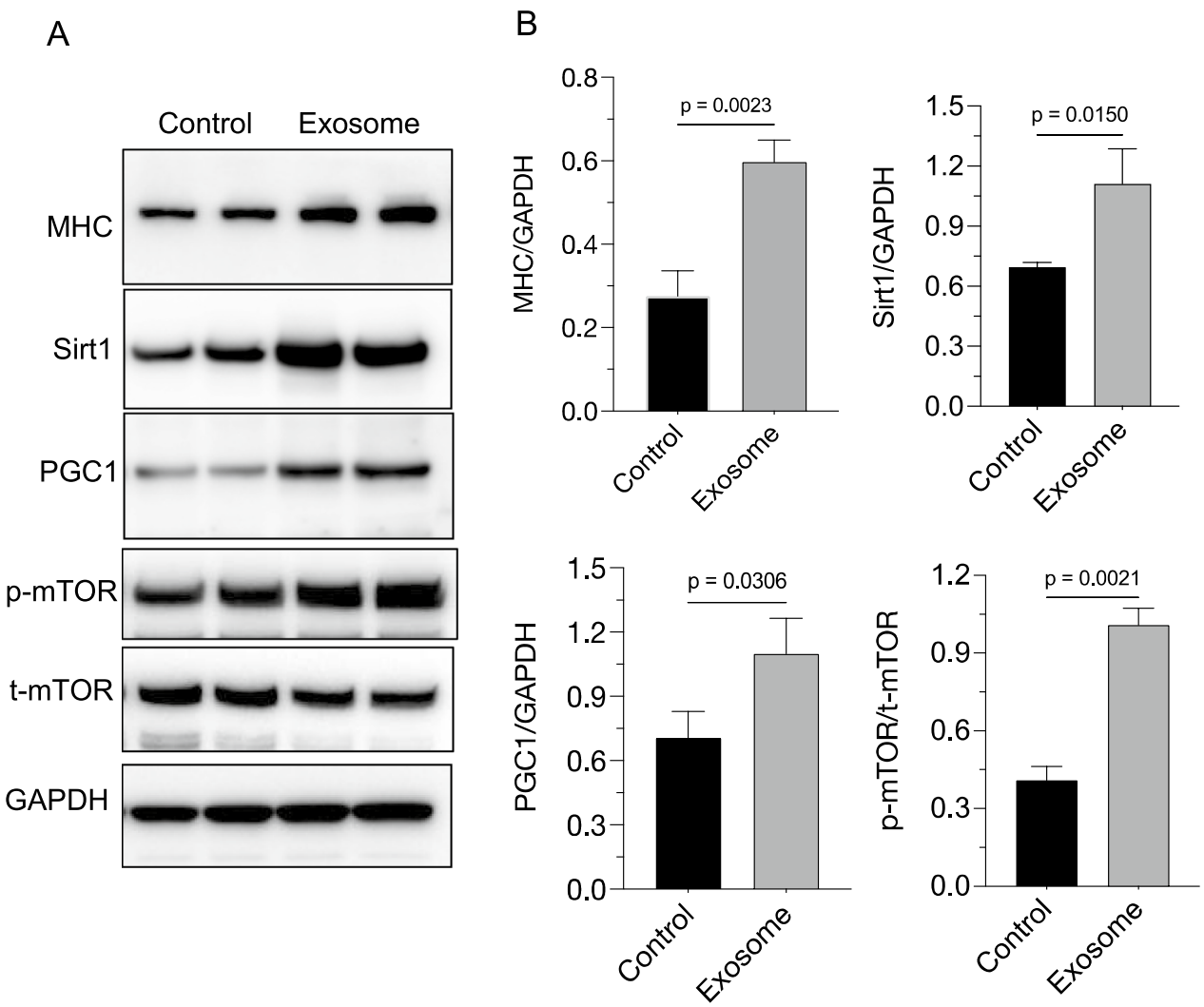

Fig. 7 HucMSC-Exos treatment reverses the harmful changes in the investigated molecules in SAMP10 mice. **a**, **b** Representative immunoblots and quantitative data show the levels of targeted protein expressions (MHC, Sirt1, PGC-1α, and p-mTOR) or phosphorylations (p-Erk1/2, p-mTOR, and p-AMPKα) in the gastrocnemius muscle. The band intensities of the targeted proteins were normalized by GAPDH. Data are means ± SD (n = 4), and $*p < 0.05$, $**p < 0.01$ by Student's *t*-test (**b**)

p-Akt, p-Erk1/2, p-AMPK, and GSK3α/β) in C2C12 cells under our experimental conditions. These findings present evidence and a potential mechanistic explanation of the hucMSC-Exos-mediated prevention of skeletal muscle atrophy and dysfunction associated with the improvement of protein anabolic metabolism, cell apoptosis and senescence, and mitochondrial biogenesis (Fig. 9).

Previous studies have reported that intravenous administration of hucMSC-Exos can lower inflammation, apoptosis, and toxicity in animal models of preeclampsia [39], osteonecrosis of the femoral head [46] and ischemic liver injury [47]. We here showed that hucMSC-Exos intervention improved the endurance and grip strength of SAMP10 mice. It also increased the skeletal muscle fiber size in the of SAMP10 mice. The western blotting results revealed that hucMSC-Exos dramatically enhanced the levels of anabolism-related proteins (p-mTOR and MHC), indicating that the use of hucMSC-Exos is likely to ameliorate skeletal muscle atrophy and dysfunction via the stimulation of an mTOR-mediated protein anabolism in the aging-associated skeletal muscle atrophy of SAPM10 mice. This notion was further supported by the in vitro finding that hucMSC-Exos administration enhanced the protein anabolism-related molecular phosphorylation levels (i.e., p-Akt, p-GSK3α/β, p-mTOR, p-AMPK, and p-Erk1/2) in C2C12 cells under our experimental conditions.

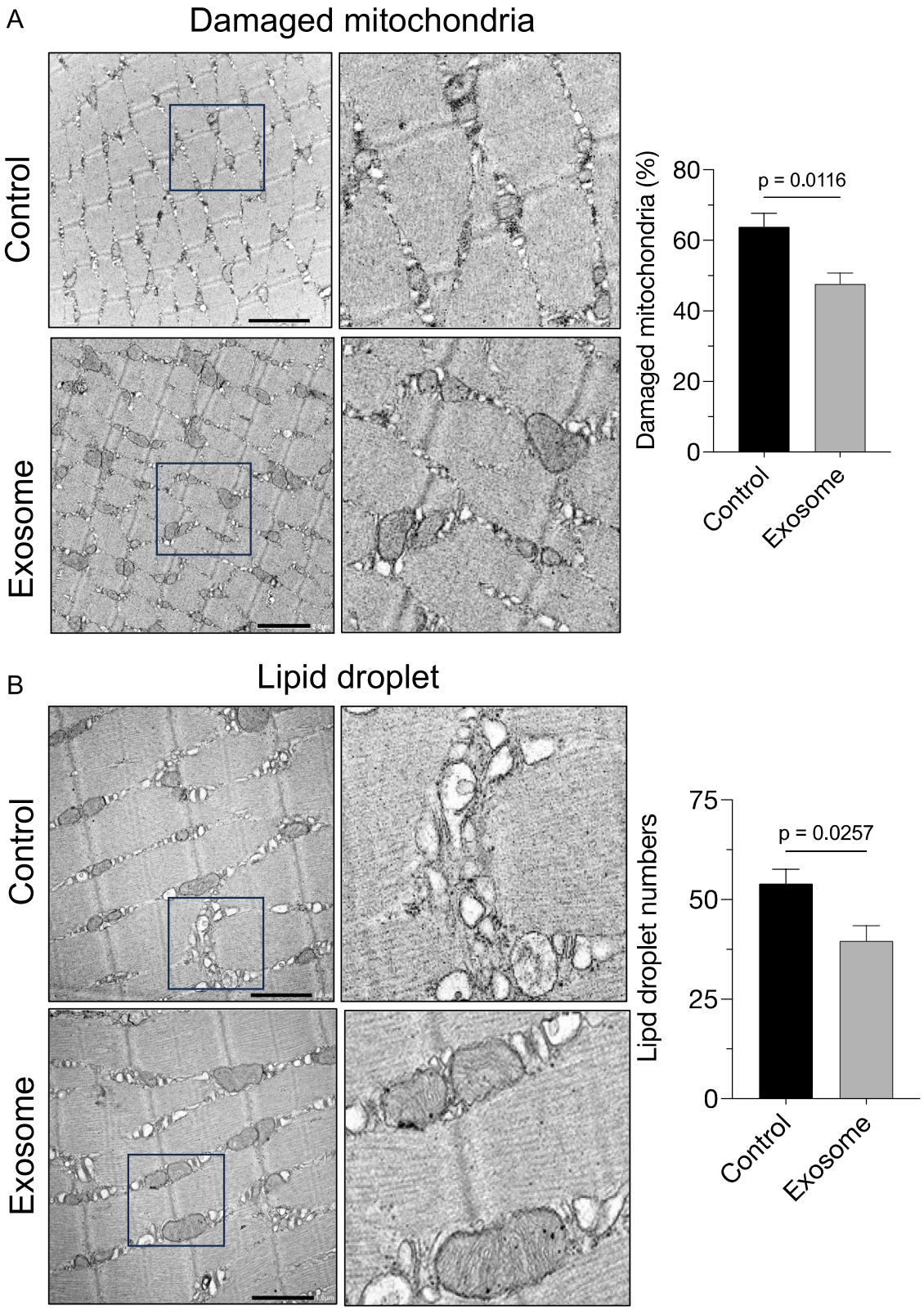

Fig. 8 hucMSC-Exos improved mitochondrial damage and lipid droplet accumulation in the gastrocnemius muscles of SAMP10 mice. **a, b** Representative electron microscopy images and quantitative data show the percentages of the damaged mitochondria and the numbers of lipid droplets in both experimental groups. Data are means ± SD (n = 4), and *p* values were determined by Student's *t*-test (**b**)

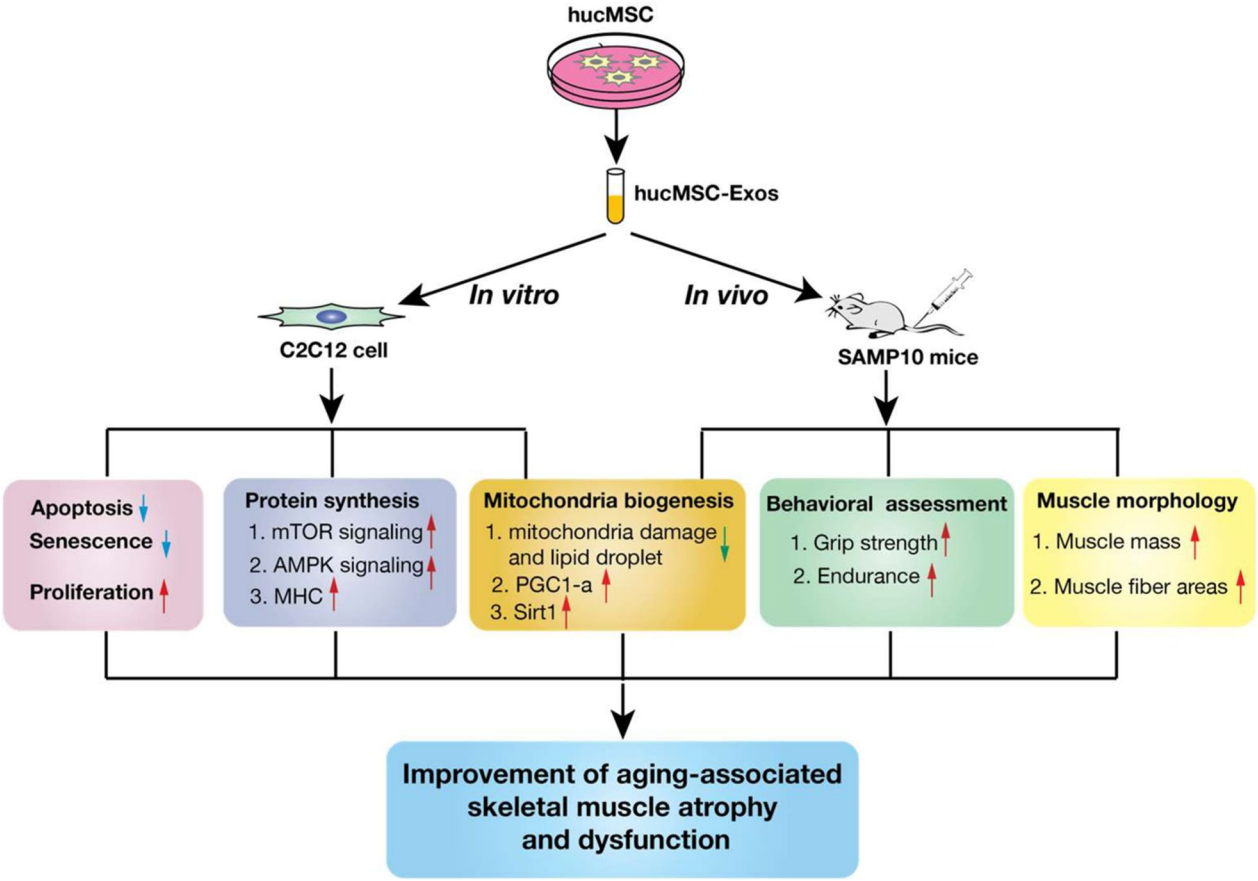

Fig. 9 Graphical illustration of hucMSC-Exos-mediated alleviation of aging-associated skeletal muscle mass loss and dysfunction in SAMP10 mouse model. These findings present evidence and a potential mechanistic explanation of the hucMSC-Exos-mediated prevention of skeletal muscle atrophy and dysfunction associated with the improvement of protein anabolic metabolism, cell apoptosis and senescence, and mitochondrial biogenesis

It is known that the skeletal muscle is a mitochondrion-rich tissue. Stimulation of mitochondrial biogenesis enhances skeletal muscular strength. [48] It is well-known that PGC1α regulates mitochondrial biogenesis via the modulation of mitochondrial nuclear gene transcription. [49] In accordance with the experimental evidence suggesting that PGC1-α expression is decreased in aged skeletal muscle tissues [5, 50], we speculated that the hucMSC-Exos-mediated benefit observed in SAMP10 mice in our experiments was likely due to increased PGC-1α activity. We observed that hucMSC-Exos treatment not only enhanced PGC1α expression but also prevented lipid droplet accumulation and mitochondrial injury of the gastrocnemius muscles in SAMP10 mice. It is known that activation of the Sirt1/PGC 1α axis can protect against mitochondrial dysfunction in isoproterenol-induced myocardial injury [51]. We have shown that hucMSC-Exos increased p-mTOR, Sirt1, and PGC1α in muscle tissues and in C2C12 lysates; and p-mTOR inhibitor rapamycin diminished these effects. Thus, the stimulation of mTOR-Sirt1/PGC1α-mediated mitochondrial biogenesis by hucMSC-Exos might has a salutary effect on the muscle dysfunction in SAMP10 mice. However, further experiments are needed to validate these pathways using inhibitors or knockdown models in vivo and in vitro.

In agreement with a previous report in which hucMSC-Exos inhibited cell apoptosis in a liver ischemic/reperfusion injury model [52], our in vitro TUNEL analysis revealed that the levels of oxidative stress-induced C2C12 cells were markedly lowered by hucMSC-Exos treatment. The western blotting analysis demonstrated that hucMSC-Exos rectified the harmful changes in Bax and Bcl-2 protein levels in C2C12 cells under hydrogen peroxide conditions. Recently, we demonstrated that human umbilical cord-derived MSCs can suppress muscle apoptosis association with a reduction of oxidative stress production and apoptosis-related protein changes (cleaved caspase-3 and −8) in the soleus and gastrocnemius muscles of SAMP10 mice [16]. Taken together,

our findings suggest that hucMSC-Exos protects skeletal muscle cells against apoptosis and thereby prevents aging-related skeletal muscle atrophy and dysfunction in mice under our experimental conditions.

This study had several limitations. First, accumulating clinical and laboratory evidence suggests that it is difficult for intravenously injected hucMSC-Exos to locate and engraft in skeletal muscles, and we were not able to apply a green fluorescent protein-labeled method or representative bioluminescence overlay images to monitor whether the hucMSC-Exos were grafted into the diseased skeletal muscle in our in vivo experiments. Second, we could not gain direct evidence of whether and where the hucMSC-Exos facilitate skeletal muscle cell differentiation in mice. Third, we did not fully examine the hucMSC-Exos-mediated muscle benefit on type I and II myofibers in soleus and gastrocnemius muscles. Fourth, we could not explore whether hucMSC-Exos treatment still confer masculoprotective actions beyond the 12-week treatment period. In addition, because of our study lacking a placebo-treated aged control group (e.g., aged untreated SAMP10 mice receiving a vehicle injection), it challenging to not fully isolate the effect of hucMSC-Exos from normal aging processes. And we also could not perform direct genetic or pharmacological inhibition studies to further validate these signaling pathways as essential mediators of hucMSC-Exos function. Finally, we did not design experiments to examine the magnitude of the biochemical, morphological, and functional deficiencies between normal healthy and SAMP10 tissue. Further experimental studies are needed to explore these issues.

On the other hand, it should be noted clinical and experimental investigations reported studies of MSC using different methods of isolation and expansion, and different approaches to characterizing the cells [53]. A comprehensive review article highlighted changes occurring in MSC secretome following the switch from healthy to senescence status. [54] it has been reported in 2009 that a large multicenter phase III clinical trial (NCT00366145) performed in the USA examining the use of an industrial MSC product failed to show its clinical endpoint of achieving a dramatic enhance of full response of steroid-resistant graft-versus-host disease (GVHD) compared with placebo [55]. A systematic review and meta-analysis documented that efficacy of MSC therapy for steroid-refractory acute GADH following allogeneic hematopoietic stem cell transplantation [56]. Token together, doing hucMSCs therapy as well as hucMSC-Exos therapy should consider key variables affecting transplant efficacy include donor variability, ex vivo expansion, senescence, immunogenicity, and cryopreservation.

Conclusions

HucMSC-Exos activates mouse skeletal muscle under pathobiological conditions such as sarcopenia. We have conducted a translational study using hucMSC-Exos to contribute to the eventual development of management strategies for aging-associated skeletal muscular diseases. Our findings suggest that aging-related loss of skeletal-muscle mass can be reversed by tail intravenous administration of hucMSC-Exos, which might be due to improvements in cell viability, apoptosis, differentiation, protein anabolism, and mitochondrial biogenesis mediated by targeted intracellular signaling pathways (i.e., the Bax/Bcl-2, myogenin/Myod1, mTOR/Akt, and Sirt1/PGC1α axes). The hucMSC-Exos-induced activation of the young-skeletal muscle action should be further studied as a potential strategy to mitigate aging-dependent declines in the muscle capacities for regeneration and repair by known and unknown paracrine factors. Such preclinical studies might also lead to the therapeutic application of stem cell technology to complement or replace physical exercise or pharmacological treatment for aging individuals with frailty and sarcopenia.

Acknowledgements

We also thank H. Ajisaka and Y. Shimizu for their technical assistance.

Author contributions

ZH Conceptualization, Formal analysis, Investigation, Methodology, Writing—original draft. LP conceptualization, Formal analysis, Investigation, Data curation, Methodology. XM investigation, Methodology. AI Data curation, Methodology. HH data curation, Methodology. MK Validation, Funding acquisition, Writing—review and editing. XC conceptualization, Funding acquisition, Project administration, Supervision, Writing—original draft, Writing—review and editing. All authors read and approved the article.

Funding

This work was supported in part by grants from the National Natural Science Foundation of China (Nos. 81770485 and 82370424) and a grant from the Ministry of Education, Culture, Sports, Science, and Technology of Japan (No. 20H03574).

Availability of data and materials

(1) All data generated or analyzed during this study are included within the article. (2) All data of this study are available from the corresponding author upon request.

Declarations

Clinical trial number

Not applicable.

Ethics approval and consent to participate

The commercially available UC-MSCs used in the present in vitro and in vivo experiments were provided by the Cord Blood and Umbilical Cord Bank of the Affiliated Hospital of Institute of Medical Sciences, University of Tokyo (IMSUT CORD, Tokyo). The animal study protocol (entitled hucMSCs therapy on sarcopenia; No. 2019-0352 approved on September 9, 2019) was approved by the Institutional Animal Care and Use Committees of by the Ethics Committee of Nagoya University and performed in accordance with the Guide for the Care and Use of Laboratory Animals published by the U.S. National Institutes of Health. The work has been reported in line with the ARRIVE guidelines 2.0. The original source (IMSUT CORD, Tokyo) has confirmed that there was initial ethical approval for collection of human cells, and that the donors had

signed informed consent (please see IMSUT CORD company's website: http://imsutcord.umin.jp/baby.html). And a Material Transfer Agreement with the commercial vendor and the authors (Japanese form) available from the corresponding author upon request.

Consent for publication
All authors agree to publish this version of the article.

Artificial intelligence
The authors declare that they have not use AI-generated work in this manuscript.

Competing interests
The authors declare that they have no conflicts of interest to disclose with respect to this manuscript.

Author details
[1]Department of Human Life Cord Applied Cell Therapy, Nagoya University Graduate School of Medicine, Nagoya, Aichi-Ken 466-8550, Japan. [2]Department of Neurology, University of Occupational and Environmental Health School of Medicine, Kitakyushu, Fukuoka 807-8555, Japan. [3]Department of Cardiology and Hypertension, Jilin Provincial Key Laboratory of Stress and Cardiovascular Disease, Yanbian University Hospital, Yanji 133000, Jilin, People's Republic of China. [4]Department of Vascular Surgery, The Second Affiliated Hospital, Zhejiang University School of Medicine, Hangzhou 310000, Zhejiang, People's Republic of China. [5]Institute of Innovation for Future Society, Nagoya University Graduate School of Medicine, Nagoya, Aichi-Ken 466-8550, Japan. [6]Department of Community Health and Geriatrics, Nagoya University Graduate School of Medicine, Nagoya 466-8550, Japan. [7]Technology Development Team, Research and Development Group, Human Life CORD Japan Inc., Tokyo 103-0012, Japan. [8]Meitetsu Hospital, Nagoya, Aichi 451-8511, Japan. [9]Division of Cardiovascular, Department of Internal Medicine, Kyung Hee University Hospital, Kyung Hee University, Seoul 130702, Korea.

Received: 11 February 2025 Accepted: 18 June 2025
Published: 28 July 2025

References

1. Jensen GL, Cederholm T. Exploring the intersections of frailty, sarcopenia, and cachexia with malnutrition. Nutr Clin Pract. 2024;39:1286–91. https://doi.org/10.1002/ncp.11180.
2. Karakousis ND, Pyrgioti EE, Georgakopoulos PN, Papanas N. Sarcopenia, frailty and diabetic foot: a mini narrative review. Int J Low Extrem Wounds. 2024;23:499–503. https://doi.org/10.1177/15347346221111420.
3. Peake J, Della Gatta P, Cameron-Smith D. Aging and its effects on inflammation in skeletal muscle at rest and following exercise-induced muscle injury. Am J Physiol Regul Integr Comput Physiol. 2010;298:R1485-1495. https://doi.org/10.1152/ajpregu.00467.2009.
4. Arthur ST, Cooley ID. The effect of physiological stimuli on sarcopenia; impact of Notch and Wnt signaling on impaired aged skeletal muscle repair. Int J Biol Sci. 2012;8:731–60. https://doi.org/10.7150/ijbs.4262.
5. Inoue A, Cheng XW, Huang Z, Hu L, Kikuchi R, Jiang H, Piao L, Sasaki T, Itakura K, Wu H, et al. Exercise restores muscle stem cell mobilization, regenerative capacity and muscle metabolic alterations via adiponectin/AdipoR1 activation in SAMP10 mice. J Cachexia Sarcopenia Muscle. 2017;8:370–85. https://doi.org/10.1002/jcsm.12166.
6. Li L, Guan X, Huang Y, Qu B, Yao B, Ding H. Identification of key genes and signaling pathways based on transcriptomic studies of aerobic and resistance training interventions in sarcopenia in SAMP8 mice. Sports Med Health Sci. 2024;6:358–69. https://doi.org/10.1016/j.smhs.2024.01.005.
7. Ferrari L, Bochicchio G, Bottari A, Scarton A, Cavedon V, Milanese C, Lucertini F, Pogliaghi S. Feasibility and effectiveness of a 6-month, home-based, resistance exercise delivered by a remote technological solution in healthy older adults. Arch Gerontol Geriatr. 2024;127: 105559. https://doi.org/10.1016/j.archger.2024.105559.
8. Flack KD, Davy KP, Hulver MW, Winett RA, Frisard MI, Davy BM. Aging, resistance training, and diabetes prevention. J Aging Res. 2010;2011: 127315. https://doi.org/10.4061/2011/127315.
9. Sun R, Wan J, Tang J, Deng Y, Zhang M, Liu C, Li J, Zhang Q. Effectiveness of resistance training on body composition, muscle strength, and biomarker in sarcopenic older adults: a meta-analysis of randomized controlled trials. Arch Gerontol Geriatr. 2025;128: 105595. https://doi.org/10.1016/j.archger.2024.105595.
10. Fujie S, Horii N, Kajimoto H, Yamazaki H, Inoue K, Iemitsu K, Uchida M, Arimitsu T, Shinohara Y, Sanada K, et al. Impact of resistance training and chicken intake on vascular and muscle health in elderly women. J Cachexia Sarcopenia Muscle. 2024. https://doi.org/10.1002/jcsm.13572.
11. Yu Y, Jiang X, Yu T, Chen F, Huang R, Xun Z, Wang X, Liu X, Xie X, Sun C, et al. Maintaining myoprotein and redox homeostasis via an orally recharged nanoparticulate supplement potentiates sarcopenia treatment. Biomaterials. 2025;314: 122863. https://doi.org/10.1016/j.biomaterials.2024.122863.
12. Theodorakis N, Feretzakis G, Vamvakou G, Verykios VS, Polymeris A, Nikolaou M. Testosterone therapy for functional hypogonadism in middle-aged and elderly males: current evidence and future perspectives. Hormones (Athens). 2024;23:801–17. https://doi.org/10.1007/s42000-024-00587-2.
13. Mendes C, Carvalho M, Bravo J, Martins S, Raimundo A. Possible interaction between physical exercise and leptin and ghrelin changes following Roux-en-Y gastric bypass in sarcopenic obesity patients-a pilot study. Nutrients. 2024. https://doi.org/10.3390/nu16223913.
14. Linard C, Brachet M, L'Homme B, Strup-Perrot C, Busson E, Bonneau M, Lataillade JJ, Bey E, Benderitter M. Long-term effectiveness of local BM-MSCs for skeletal muscle regeneration: a proof of concept obtained on a pig model of severe radiation burn. Stem Cell Res Ther. 2018;9:299. https://doi.org/10.1186/s13287-018-1051-6.
15. Tang X, Zheng N, Lin Q, You Y, Gong Z, Zhuang Y, Wu J, Wang Y, Huang H, Ke J, et al. Hypoxia-preconditioned bone marrow-derived mesenchymal stem cells protect neurons from cardiac arrest-induced pyroptosis. Neural Regen Res. 2025;20:1103–23. https://doi.org/10.4103/nrr.Nrr-d-23-01922.
16. Piao L, Huang Z, Inoue A, Kuzuya M, Cheng XW. Human umbilical cord-derived mesenchymal stromal cells ameliorate aging-associated skeletal muscle atrophy and dysfunction by modulating apoptosis and mitochondrial damage in SAMP10 mice. Stem Cell Res Ther. 2022;13:226. https://doi.org/10.1186/s13287-022-02895-z.
17. Trapana J, Weinerman J, Lee D, Sedani A, Constantinescu D, Best TM, Hornicek FJ Jr, Hare JM. Cell-based therapy in the treatment of musculoskeletal diseases. Stem Cells Transl Med. 2024;13:959–78. https://doi.org/10.1093/stcltm/szae049.
18. Hori A, Takahashi A, Miharu Y, Yamaguchi S, Sugita M, Mukai T, Nagamura F, Nagamura-Inoue T. Superior migration ability of umbilical cord-derived mesenchymal stromal cells (MSCs) toward activated lymphocytes in comparison with those of bone marrow and adipose-derived MSCs. Front Cell Dev Biol. 2024;12:1329218. https://doi.org/10.3389/fcell.2024.1329218.
19. Nagamura-Inoue T, Kato S, Najima Y, Isobe M, Doki N, Yamamoto H, Uchida N, Takahashi A, Hori A, Nojima M, et al. Immunological influence of serum-free manufactured umbilical cord-derived mesenchymal stromal cells for steroid-resistant acute graft-versus-host disease. Int J Hematol. 2022;116:754–69. https://doi.org/10.1007/s12185-022-03408-7.
20. Kalluri R, LeBleu VS. The biology, function, and biomedical applications of exosomes. Science. 2020. https://doi.org/10.1126/science.aau6977.
21. Guo R, Wu Z, Liu A, Li Q, Han T, Shen C. Hypoxic preconditioning-engineered bone marrow mesenchymal stem cell-derived exosomes promote muscle satellite cell activation and skeletal muscle regeneration via the miR-210-3p/KLF7 mechanism. Int Immunopharmacol. 2024;142: 113143. https://doi.org/10.1016/j.intimp.2024.113143.
22. Wu S, Zhang Y, Hou Y, Zhu J, Yang H, Cui Y. Research on the role of exosomes secreted by immortalized adipose-derived mesenchymal stem cells differentiated into pericytes in the repair of high glucose-induced retinal vascular endothelial cell damage. Exp Eye Res. 2024;247: 110046. https://doi.org/10.1016/j.exer.2024.110046.
23. Liu Y, Chen J, Xiong J, Hu JQ, Yang LY, Sun YX, Wei Y, Zhao Y, Li X, Zheng QH, et al. Potential cardiac-derived exosomal miRNAs involved in cardiac healing and remodeling after myocardial ischemia-reperfusion injury. Sci Rep. 2024;14:24275. https://doi.org/10.1038/s41598-024-75517-8.
24. Zhang A, Sun B, Nan C, Cong L, Zhao Z, Liu L. Effects of 3D-printed exosome-functionalized brain acellular matrix hydrogel on

neuroinflammation in rats following cerebral hemorrhage. Stem Cell Res Ther. 2025;16:196. https://doi.org/10.1186/s13287-025-04332-3.
25. Zhu H, Guo X, Zhang Y, Khan A, Pang Y, Song H, Zhao H, Liu Z, Qiao H, Xie J. The combined anti-aging effect of hydrolyzed collagen oligopeptides and exosomes derived from human umbilical cord mesenchymal stem cells on human skin fibroblasts. Molecules. 2024. https://doi.org/10.3390/molecules29071468.
26. Sun X, Mao Y, Liu B, Gu K, Liu H, Du W, Li R, Zhang J. Mesenchymal stem cell-derived exosomes enhance 3D-printed scaffold functions and promote alveolar bone defect repair by enhancing angiogenesis. J Pers Med. 2023. https://doi.org/10.3390/jpm13020180.
27. Yang J, Chen Z, Pan D, Li H, Shen J. Umbilical Cord-derived mesenchymal stem cell-derived exosomes combined pluronic F127 hydrogel promote chronic diabetic wound healing and complete skin regeneration. Int J Nanomed. 2020;15:5911–26. https://doi.org/10.2147/ijn.S249129.
28. Meng X, Huang Z, Inoue A, Wang H, Wan Y, Yue X, Xu S, Jin X, Shi GP, Kuzuya M, et al. Cathepsin K activity controls cachexia-induced muscle atrophy via the modulation of IRS1 ubiquitination. J Cachexia Sarcopenia Muscle. 2022;13:1197–209. https://doi.org/10.1002/jcsm.12919.
29. Yue X, Piao L, Wang H, Huang Z, Meng X, Sasaki T, Inoue A, Nakamura K, Wan Y, Xu S, et al. Cathepsin K deficiency prevented kidney damage and dysfunction in response to 5/6 nephrectomy injury in mice with or without chronic stress. Hypertension. 2022;79:1713–23. https://doi.org/10.1161/hypertensionaha.122.19137.
30. Lin Z, Zhao M, Zhang X, Piao J, Zheng X, Shu S, Zhao L, Zhang M, Shi GP, Lei Y, et al. CD8+ T-cell deficiency protects mice from abdominal aortic aneurysm formation in response to calcium chloride2. J Hypertens. 2024. https://doi.org/10.1097/hjh.0000000000003823.
31. Xu S, Piao L, Wan Y, Huang Z, Meng X, Inoue A, Wang H, Yue X, Jin X, Shi GP, et al. CTSS modulates stress-related carotid artery thrombosis in a mouse FeCl(3) model. Arterioscler Thromb Vasc Biol. 2023;43:e238–53. https://doi.org/10.1161/atvbaha.122.318455.
32. Xue QL. The frailty syndrome: definition and natural history. Clin Geriatr Med. 2011;27:1–15. https://doi.org/10.1016/j.cger.2010.08.009.
33. Alessio N, Aprile D, Cappabianca S, Peluso G, Di Bernardo G, Galderisi U. Different stages of quiescence, senescence, and cell stress identified by molecular algorithm based on the expression of Ki67, RPS6, and beta-galactosidase activity. Int J Mol Sci. 2021;22:234. https://doi.org/10.3390/ijms22063102.
34. Zhang M, Yue X, Xu S, Piao J, Zhao L, Shu S, Kuzuya M, Li P, Hong L, Kim W, et al. Dipeptidyl peptidase-4 disturbs adipocyte differentiation via the negative regulation of the glucagon-like peptide-1/adiponectin-cathepsin K axis in mice under chronic stress conditions. Faseb J. 2024;38: e23684. https://doi.org/10.1096/fj.202400158R.
35. Wan Y, Piao L, Xu S, Meng X, Huang Z, Inoue A, Wang H, Yue X, Jin X, Nan Y, et al. Cathepsin S activity controls chronic stress-induced muscle atrophy and dysfunction in mice. Cell Mol Life Sci. 2023;80:254. https://doi.org/10.1007/s00018-023-04888-4.
36. Wan Y, Piao L, Xu S, Inoue A, Meng X, Lei Y, Huang Z, Wang H, Yue X, Shi GP, et al. Cathepsin S deficiency improves muscle mass loss and dysfunction via the modulation of protein metabolism in mice under pathological stress conditions. Faseb J. 2023;37: e23086. https://doi.org/10.1096/fj.202300395RRR.
37. Fang J, Shu S, Dong H, Yue X, Piao J, Li S, Hong L, Cheng XW. Histone deacetylase 6 controls cardiac fibrosis and remodelling through the modulation of TGF-β1/Smad2/3 signalling in post-infarction mice. J Cell Mol Med. 2024;28: e70063. https://doi.org/10.1111/jcmm.70063.
38. Kang J, Guo Y. Human umbilical cord mesenchymal stem cells derived exosomes promote neurological function recovery in a rat spinal cord injury model. Neurochem Res. 2022;47:1532–40. https://doi.org/10.1007/s11064-022-03545-9.
39. Sun J, Zhang W. Huc-MSC-derived exosomal miR-144 alleviates inflammation in LPS-induced preeclampsia-like pregnant rats via the FosB/Flt-1 pathway. Heliyon. 2024;10: e24575. https://doi.org/10.1016/j.heliyon.2024.e24575.
40. Wu X, Zeng Z, Peng K, Ren D, Zhang L. Regulatory mechanism of DHRS2-modified human umbilical cord mesenchymal stem cells-derived exosomes in prostate cancer cell proliferation and apoptosis. Tissue Cell. 2023;82: 102078. https://doi.org/10.1016/j.tice.2023.102078.
41. Wang JF, Wen DT, Wang SJ, Gao YH, Yin XY. Muscle-specific overexpression of Atg2 gene and endurance exercise delay age-related deteriorations of skeletal muscle and heart function via activating the AMPK/Sirt1/PGC-1α pathway in male Drosophila. Faseb J. 2023;37: e23214. https://doi.org/10.1096/fj.202301312R.
42. Sanz-Nogués C, Keane AJ, Creane M, Hynes SO, Chen X, Lyons CJ, Horan E, Elliman SJ, Goljanek-Whysall K, O'Brien T. Mesenchymal stromal cell transplantation ameliorates fibrosis and microRNA dysregulation in skeletal muscle ischemia. Stem Cells. 2024;42:976–91. https://doi.org/10.1093/stmcls/sxae058.
43. Świątkowska-Flis B, Zdolińska-Malinowska I, Sługocka D, Boruczkowski D. The use of umbilical cord-derived mesenchymal stem cells in patients with muscular dystrophies: Results from compassionate use in real-life settings. Stem Cells Transl Med. 2021;10:1372–83. https://doi.org/10.1002/sctm.21-0027.
44. Fang S, Xu C, Zhang Y, Xue C, Yang C, Bi H, Qian X, Wu M, Ji K, Zhao Y, et al. Umbilical cord-derived mesenchymal stem cell-derived exosomal microRNAs suppress myofibroblast differentiation by inhibiting the transforming growth factor-β/SMAD2 pathway during wound healing. Stem Cells Transl Med. 2016;5:1425–39. https://doi.org/10.5966/sctm.2015-0367.
45. Klimczak A, Kozlowska U, Kurpisz M. Muscle stem/progenitor cells and mesenchymal stem cells of bone marrow origin for skeletal muscle regeneration in muscular dystrophies. Arch Immunol Ther Exp (Warsz). 2018;66:341–54. https://doi.org/10.1007/s00005-018-0509-7.
46. Tang Z, Xu X, Shi W, Ren X, Luo H, Xu Y, Li C. Huc-MSC-derived exosomes alleviates alcohol-induced osteonecrosis of the femoral head through targeting the miR-25-3p/GREM1 axis. Genomics. 2025. https://doi.org/10.1016/j.ygeno.2025.110996.
47. Sameri MJ, Savari F, Hoseinynejad K, Danyaei A, Mard SA. The hepatoprotective effect of H2S-modified and non-modified mesenchymal stem cell exosomes on liver ischemia-reperfusion injury in mice: the role of MALAT1. Biochem Biophys Res Commun. 2022;635:194–202. https://doi.org/10.1016/j.bbrc.2022.09.111.
48. Sun S, Yu T, Huh JY, Cai Y, Yoon S, Javaid HMA. *Aminoguanidine hemisulfate* improves mitochondrial autophagy, oxidative stress, and muscle force in Duchenne muscular dystrophy via the AKT/FOXO1 pathway in mdx mice. Skelet Muscle. 2025;15:2. https://doi.org/10.1186/s13395-024-00371-1.
49. Dobashi S, Yoshihara T, Ogura Y, Naito H. Normobaric hypoxia accelerates high-intensity intermittent training-induced mitochondrial biogenesis (PGC-1α)- and dynamics (OPA1)-related protein expressions in rat gastrocnemius muscle. J Physiol Biochem. 2024;80:909–17. https://doi.org/10.1007/s13105-024-01052-9.
50. Fu Y, Tao L, Wang X, Wang B, Qin W, Song L. PGC-1α participates in regulating mitochondrial function in aged sarcopenia through effects on the Sestrin2-mediated mTORC1 pathway. Exp Gerontol. 2024;190:112428. https://doi.org/10.1016/j.exger.2024.112428.
51. Naaz S, Mishra S, Pal PK, Chattopadhyay A, Das AR, Bandyopadhyay D. Activation of SIRT1/PGC 1α/SIRT3 pathway by melatonin provides protection against mitochondrial dysfunction in isoproterenol induced myocardial injury. Heliyon. 2020;6: e05159. https://doi.org/10.1016/j.heliyon.2020.e05159.
52. Zhang L, Song Y, Chen L, Li D, Feng H, Lu Z, Fan T, Chen Z, Livingston MJ, Geng Q. MiR-20a-containing exosomes from umbilical cord mesenchymal stem cells alleviates liver ischemia/reperfusion injury. J Cell Physiol. 2020;235:3698–710. https://doi.org/10.1002/jcp.29264.
53. Dominici M, Le Blanc K, Mueller I, Slaper-Cortenbach I, Marini F, Krause D, Deans R, Keating A, Prockop D, Horwitz E. Minimal criteria for defining multipotent mesenchymal stromal cells. The International Society for Cellular Therapy position statement. Cytotherapy. 2006;8:315–7. https://doi.org/10.1080/14653240600855905.
54. Siraj Y, Galderisi U, Alessio N. Senescence induces fundamental changes in the secretome of mesenchymal stromal cells (MSCs): implications for the therapeutic use of MSCs and their derivates. Front Bioeng Biotechnol. 2023;11:1148761. https://doi.org/10.3389/fbioe.2023.1148761.
55. Galipeau J. The mesenchymal stromal cells dilemma–does a negative phase III trial of random donor mesenchymal stromal cells in steroid-resistant graft-versus-host disease represent a death knell or a bump in

the road? Cytotherapy. 2013;15:2–8. https://doi.org/10.1016/j.jcyt.2012.10.002.
56. Chen X, Wang C, Yin J, Xu J, Wei J, Zhang Y. Efficacy of mesenchymal stem cell therapy for steroid-refractory acute graft-versus-host disease following allogeneic hematopoietic stem cell transplantation: a systematic review and meta-analysis. PLoS ONE. 2015;10: e0136991. https://doi.org/10.1371/journal.pone.0136991.

Publisher's Note